

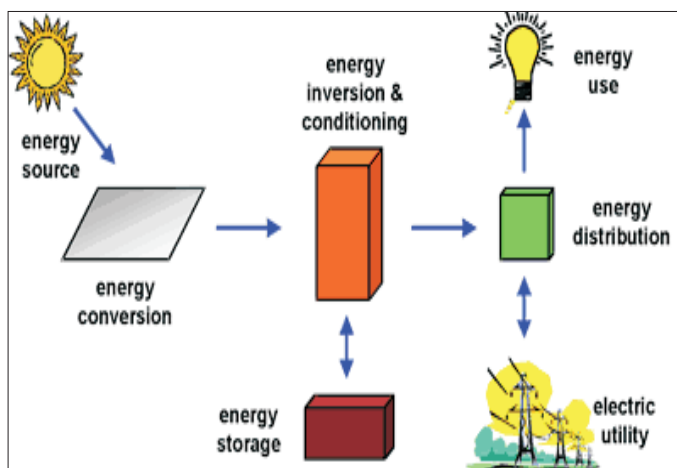
## MITIGATION OF VOLTAGE FLUCTUATION UNDER FAULTLY CONDITIONS BY USING DYNAMIC VOLTAGE RESTORER WITH INTEGRATED PHOTOVOLTAIC SYSTEM

<sup>1</sup>S. Sai Kumar, <sup>2</sup>S. Sujatha Devi, <sup>3</sup>T. Srinivasarao

<sup>1</sup>M.Tech Student, <sup>2</sup>Assistant Professor, <sup>3</sup>HOD & Associate Professor

<sup>1,2,3</sup>Department of Electrical & Electronics Engg.,

Avanathi Insitute of Engg.&Tech., Narsipatnam. Andra Pradesh.



### ABSTRACT

With the accelerated penetration of sensitive loads, the vigor satisfactory disorders within the distribution method have drastically increased majorly in renewable vigour resources. A new methodology for integrating a grid connected photovoltaic method in conjunction with self-supported dynamic voltage restorer (DVR) is introduced and its important perform is to inject active power through maximum power point monitoring(MPPT) manipulate of pv array and similarly to maintain uninterrupted voltage at load

terminals among which DVR is considered as most potent and comprehensive answer. On this projected process complete of 9 semiconductor switches termed as six-port converter. Furthermore, this configuration allows bidirectional energetic vigour flow between six-port converter and utility grid. A particular learn on all feasible operational modes together with manipulate algorithm is developed. The legitimacy of the proposed configuration is validated by means of wide simulation as well as experimental reports below exceptional working stipulations. With the MATLAB centered historical past you may design this new DVR configuration together with PV much faster and design shall be more targeted.

**KEYWORDS:** –Bidirectional power flow, Distributed power generation, Photovoltaic (PV) systems, Power quality, Voltage control.

### INTRODUCTION

The speedy depletion of conventional vigour resources and increasing environmental considerations have made renewable energy resources, such as photovoltaic (PV) and wind, innovative sources of electrical vigor new release. On the grounds that vigor generated by a PV supply is principally dc, it requires a dc-ac inversion stage for grid-linked operation. The fundamental component of a grid-connected PV procedure is more often than not the three section voltage source inverter (VSI) having six switches in complete. Its foremost function is to increase the injected energetic vigor by means of highest

vigour point tracking (MPPT) manipulate of PV array . Then again, with the extended penetration of sensitive masses, the energy best problems within the cutting-edge distribution method have greatly elevated [6]. Most standard and severe disturbances in the grid voltage are sags, swells, and faults. To maintain uninterrupted voltage at load terminals, more than a few custom power contraptions are used amongst which DVR is regarded as probably the most potent and comprehensive answer.

It's likely that the ultra-modern load facilities would be prepared with on-website online PV new release unit(s) as good as customized vigor device(s) for critical load security. This indicates this type of process configuration the place a grid-related PV plant injects active vigor via six-switch VSI (PV-VSI) while self-supported DVR performs voltage sag compensation for sensitive masses utilizing second six-swap VSI (DVR-VSI). Throughout the occurrence of fault/deep sag on the point of fashioned coupling (PCC), these unbiased PV and DVR methods face primary operational limitations. In this situation, the self-supported DVR can no longer keep the rated load voltage as a result of finite vigor in dc-link capacitor. In a similar fashion, the lively power produced by using PV plant can't be offered to the grid. One viable answer for DVR is to hold the dc-hyperlink capacitor charged at rated price through a shunt rectifier connected at load side. Nonetheless, this con-figuration faces giant VA loading of DVR-VSI, which ought to be rated for each load and shunt rectifier VA. An extra approach to increase the DVR performance is to switch the dc-hyperlink capacitor with a battery power storage process. Even it does no longer have an effect on DVR rating but incurs further battery preservation disorders.

The VA ranking of centralized PV inverter is determined by the set up ability of PV sun panels. This inverter VA is most of the time underutilized as a result of intermittent nature of sunlight vigor specifically during late evening hours, night time hours, and early morning hours the place it remains idle. Then again, the DVR VA score is by and large 20%–forty% of the complete load VA loading. The DVR inverter also has low-utilization element because the voltage disturbance is a brief duration vigor best obstacle and does now not occur traditionally. The proposed multi loop control system provides a desirable transient response and steady-state performance and effectively damps the potential resonant oscillations caused by the DVR LC harmonic filter. By combining the above two applications, in this paper, a new six-port converter-based system configuration is proposed for integrating on-site PV generation unit and DVR as shown in Fig. 2. The proposed configuration eliminates the requirement of two separate inverters for PV and DVR application reduce the switch count of conventional system by 25% and most importantly overcomes the above-mentioned operational limitations associated with conventional PV and DVR systems. The proposed configuration could be useful for low to medium power load centers/factories with sensitive loads and consider onsite PV generation capacity (more than 50% of the load requirement). Under this consideration, the VA rating of PV system will govern the overall VA rating of six-port Converter, which means that equally rated (as of PV system), DVR is available for load voltage regulation.

In the literature, the six-port converter is reported as a replacement of traditional back to back converters for dual motor drives , rectifier–inverter systems , uninterrupted power supplies UPQC and for micro grid applications . Fault ride through enhancement of DFIG–based wind energy conversion system using nine switch-based converters is also reported recently. Nevertheless, the proposed configuration of Fig. 2 retains all the essential features of traditional 12 switch system in Fig. 1. It replaces the two dissimilar VSIs with one integrated converter while reducing the overall semiconductor count, gate drive, and control circuitry (by 25%). Furthermore, the configuration allows bidirectional active power flow between six-port converter, PV plant, and utility grid, a feature that provides seamless sag compensation to protect sensitive loads during severe voltage dips at PCC. The proposed work is evaluated by detailed simulation study and finally, validated experimentally.

**II. PROPOSED CONFIGURATION AND CONTROL STRATEGY**  
**PROPOSED INTEGRATED PV- DVR SYSTEM**

The proposed system configuration is shown in Fig. 2. In this configuration, nine semiconductor switches are used to realize PV and DVR operations simultaneously. The main difference between the proposed configuration and the system given in Fig. 1 is the dual output six-port converter whose six outputs are divided into two set of outputs. The left three ports {a, b, c} connected to PCC are designated as the output of PV-VSI, whereas the right three ports {x, y, z} are designated as out-put of DVR-VSI. Switches S4 –S6 are shared between PV and DVR VSIs. Based on the grid condition and PV plant status, the six-port converter can operate in one of the various operational modes as given in Table I.

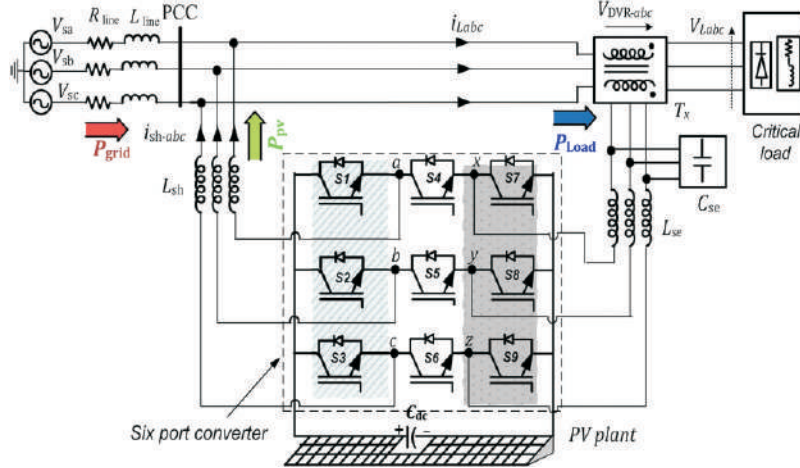


Fig 1: Proposed Configuration of PV with DVR.

**INTERLEAVING TECHNIQUE WITH DIFFERENT OPERATING MODES ACTION OF DVR:**

The main function of a DVR is the protection of sensitive loads from voltage sags/swells coming from the network. The DVR is located on approach of sensitive loads. If a fault occurs on other lines, DVR inserts series voltage VDVR and compensates load voltage to pre fault value. The momentary amplitudes of the three injected phase voltages are controlled such as to eliminate any detrimental effects of a bus fault to the load voltage VL. This means that any differential voltages caused by transient disturbances in the ac feeder will be compensated by an equivalent voltage generated by the converter and injected on the medium voltage level through the booster transformer. The DVR works independently of the type of fault or any event that happens in the system, provided that the whole system remains connected to the supply grid, i.e. the line breaker does not trip. For most practical cases, a more economical design can be achieved by only compensating the positive and negative sequence components of the voltage disturbance seen at the input of the DVR. This option is Reasonable because for a typical distribution bus configuration, the zero sequence part of a disturbance will not pass through the step down transformer because of infinite impedance for this component.

The DVR has two modes of operation which are: standby mode and boost mode. In standby mode (VDVR=0), the booster transformer’s low voltage winding is shorted through the converter. No switching of semiconductors occurs in this mode of operation, because the individual converter legs are triggered such as to establish a short-circuit path for the transformer connection. Therefore, only the comparatively low conduction losses of the semiconductors in this current loop contribute to the losses. The DVR will be most of the time in this mode. In boost mode (VDVR>0) the DVR is injecting a compensation voltage through the booster transformer due to a detection of a supply voltage disturbance.

**A. HEALTHY MODE:**

Mode-1 reflects the normal operation of six-port converter when the grid voltage is at nominal value and PV plant is operating at standard atmospheric condition (SAC). During Mode-1, PV-VSI injects the active power generated by PV plant in the grid while DVR-VSI remains inactive as the grid is healthy. Fig. 3 shows the equivalent operational circuit of six-port converter depicting the status of each switch. The carrier-based modulation scheme (further explained in Section III) generates the necessary gating signal pattern for all the switches. As shown in Fig. 3 and Table I, switches S7 –S9 are “ON (logical high)” throughout Mode-1 while remaining six switches (S1 –S6) are operated in pulse width modulation (PWM) control to perform PV-VSI operation. The ON status of S7 –S9 effectively short circuits the primary windings of series injection transformer and thus, the active power supplied by DVR-VSI ( $P_{dvr-vsi}$ ) is zero.

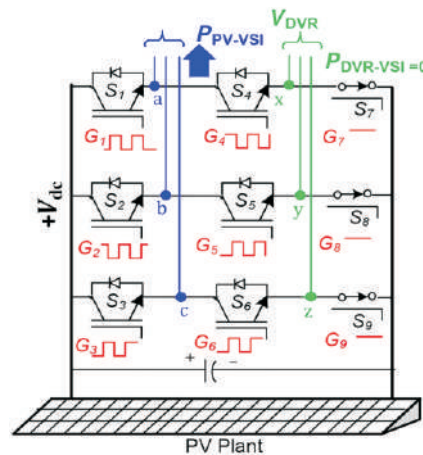


Fig.2: Equivalent Circuit Representation.

**B. FAULT MODE**

Mode-2 corresponds to a condition when there is a three-phase fault at PCC. During this mode, PV-VSI remains inactive while DVR-VSI injects the maximum compensating voltages. Critical load independently (with no support from utility grid) through the switches S4 –S9 and functions as PV supported DVR. Since the conventional PV and self-supported DVR system cannot perform during three-phase fault at PCC, Mode-2 is unique feature of the proposed configuration that cannot be realized in Fig. 1. Under such condition, the necessary neutral point for series transformer is provided through PV-VSI coupling inductor with S1 –S3 remain ON throughout. Note that there would be a small voltage drop across these inductors, which can be easily compensated by DVR itself.

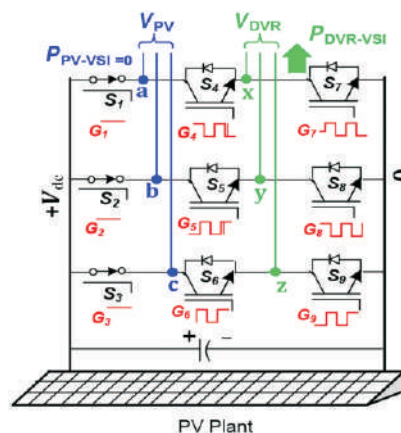


Fig.3: Fault Mode



**C. SAGMODE**

Mode-3 considers the operation of six-port converter during voltage sag at PCC. In this mode, the DVR-VSI performs the pre sag compensation to avoid premature tripping of critical load (VLabc). The gating signals for three left-most switches of six switches are due to large phase jump. Since the grid voltage is nonzero, the port converter remains at logic high. Therefore, switches S1 –S3 are “ON” throughout the Mode-2 as shown in Fig. 4. Since the PV plant is operating at SAC, the six-port converter feeds the PV plant contributes to inject limited active power based on the maximum current capacity, i.e., both DVR and PV-VSI (all nine switches) are active during Mode-3 as shown in 2.6

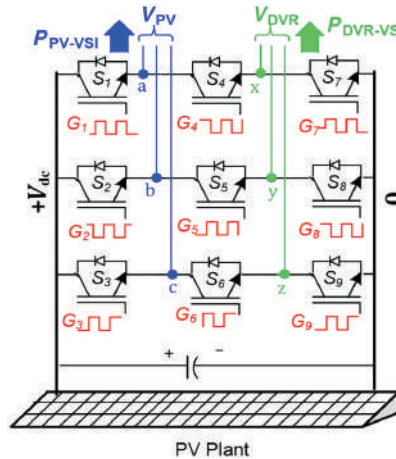


Fig.:4: Sag Mode

**D. NO PV GENERATION**

Mode-4 corresponds to the operation of six-port converter when PV plant does not provide any active power and remains inactive (during early morning hours, late evening hours, fully cloudy day, and throughout night hours). In the absence of PV plant, the role of PV-VSI is reversed. It remains idle as long as the grid is operating at rated voltage and draws active power from grid during sag intervals to keep the dc-link capacitor charged at rated value. The equivalent representation of this mode is similar to Mode-3 as shown in Fig. 6 with the modification that PV-VSI active power flow is reversed (from grid towards dc link). In the case of severe or deeper sag depths where the current requirement exceeds the switch current rating, the dc-link regulation cannot be performed. The capacitor size  $C_{dc}$  in such cases is calculated based on a equation

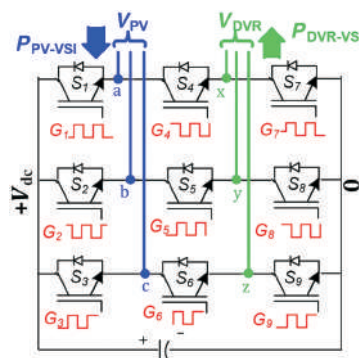


Fig.5: Equivalent System

**DIFFERENT MODES OF OPERATION:**

| Mode | PV status | Grid condition                     | Switch status |           | Six-port converter operation   |  |
|------|-----------|------------------------------------|---------------|-----------|--------------------------------|--|
|      |           |                                    | Always "ON"   | PWM       | PV-VSI                         | DVR-VSI                                    |
| 1    | Active    | Healthy<br>$V_{pcc-p.u.} = 1$      | $S_7-S_9$     | $S_1-S_6$ | Active<br>( $P_{PV-VSI} > 0$ ) | Idle<br>( $P_{DVR-VSI} = 0$ )              |
| 2    | Active    | Fault<br>$V_{pcc-p.u.} \approx 0$  | $S_1-S_3$     | $S_4-S_9$ | Idle<br>( $P_{PV-VSI} = 0$ )   | Active<br>( $P_{DVR-VSI} = P_{Q_{LOAD}}$ ) |
| 3    | Active    | Sag<br>$0.1 < V_{pcc-p.u.} < 0.95$ | None          | $S_1-S_9$ | Active<br>( $P_{PV-VSI} > 0$ ) | Active<br>( $P_{DVR-VSI} < P_{Q_{LOAD}}$ ) |
| 4    | Inactive  | Any of the above 3                 | None          | $S_1-S_9$ | Active<br>( $P_{PV-VSI} < 0$ ) | Active                                     |

**III MODULATION SCHEME FOR PROPOSED CONVERTER**

**A. SWITCHING MODES**

As shown in Fig. 2, the six-port converter has three switches shared between PV and DVR-VSIs. It, therefore, faces restriction on the allowable switching states. The two output ports on the same leg can have four possible connections. 1) Both outputs connected to +Vdc (for phase-a: S1 -ON, S4 -ON, and S7 -OFF); 2) both to 0 V (for phase-a: S1 -OFF, S4 -ON, and S7 -ON); 3) left port to +Vdc and right port to 0 V (for phase-a: S1 -ON, S4 -OFF, and S7 -ON); and 4) left port to 0 V and right port to +Vdc (for phase-a: S1 -ON, S4 -ON, and S7 -ON).

**B. COMPARISON OF SIGNAL**

The last combination, however, cannot be realized as it will result in direct short-circuiting of dc link. To achieve modulation, both the reference signals are compared with a common carrier for generating the gate pulses. In the common carrier band, the modulation reference signal of left port is placed above that of right using third harmonic injection method with no impact on output (line voltages) of six-port converter. To prevent the dc-link short circuit (due to combination 4), the crossover between two modulating reference signals should be avoided.

**C. EQUAL AND VARIABLE FREQUENCY OPERATION**

Two types of operations of six-port converter are possible to overcome the aforementioned limitation. 1) Equal frequency (EF) operation, where both set of outputs (i.e.,  $V_{pv-abc}$  and  $V_{dvr-xyz}$ ) must operate at same frequency with small inter phase difference as shown in Fig. 7(a). 2) Variable frequency (VF) operation of both set of outputs. This operation is more flexible as there is no constraint on the output frequency and could be useful for harmonic compensation [Fig. 7(b)]. However, the sum of modulation references for where  $t_{c-max}$  is the maximum compensation time.  $m_{i-max}$  is the maximum modulation index of DVR-VSI.  $n_t$  is the transformer turns ratio and  $P_{dvr-vsi}$  is the active power required to maintain the nominal load voltage. Further details on the capacitor sizing are given. Left and right port must not exceed unity. VF operation requires doubling of dc-link voltage to prevent reference crossover as shown in Fig. 7(b). Further details on these operations (EF and VF) and six-port configuration can be found below.

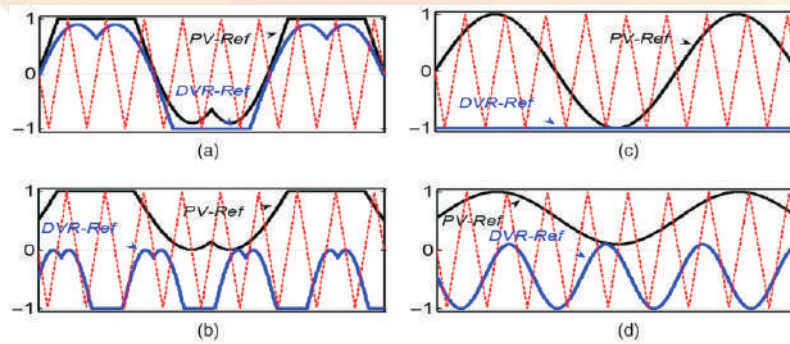


Fig.6: Per phase representation of PV and DVR-VSI modulation references during (a) EF operation; (b) VF operation; (c) healthy grid mode; and (d) sag mode.

During the normal mode, PV-VSI injects active power into grid while DVR-VSI is idle (Mode-1). The modulation index is PWM<sub>pv</sub> and PWM<sub>dvr</sub> giving two sets of six gating signals, respectively unity for PV-VSI and zero for DVR-VSI as shown in Fig. 6(c). During sag (Mode-3) the PV-VSI continues to inject active power similar to Mode-1, but at a reduced modulation index, as the PCC voltage is reduced due to voltage sag. This facilitates the DVR-VSI to attain higher modulation index (required to compensate the sag) as shown in above figure. The increase in DVR-VSI is always accomplishing decrease in PV-VSI reference and hence the crossover does not happen. Thus, the proposed configuration naturally overcomes the limitation of reference crossover. To achieve the above operation in the proposed configuration, the procedure to generate nine gate pluses is discussed below. The two reference signals can be expressed as where  $M_c$  is the carrier signal amplitude. These twelve gating signals can be directly sent to corresponding inverters if PV and DVR VSIs are operated using two separate six switch inverters like in Fig. 1. However, in the six-port converter, since the middle row switches are shared, their gate pulses are generated by logical OR operation of PWM signals corresponding to right three switches of PV-VSI, i.e., G<sub>pv4-6</sub> and left three switches of DVR-VSI, i.e., G<sub>dvr1-3</sub>. The final nine gating signals G<sub>n1-9</sub> are obtained as follows

#### IV. OVERALL CONTROL SYSTEM

The adopted DVR converter is comprised of three independent H-bridge VSCs that are connected to a common dc-link capacitor. These VSCs are series connected to the supply grid, each through a single-phase transformer. The proposed FCI control system consists of three independent and identical controllers one for each single-phase VSC of the DVR.

Assume the fundamental frequency components of the supply voltage  $V_s$ , load voltage  $V_l$ , and the injected voltage  $V_{in}$ , are two identical least error squares (LES) filters are used to estimate the magnitudes and phase angles of the phase FCI function requires a phasor parameter estimator (digital filter) which attenuates the harmonic contents of the measured signal. To attenuate all harmonics, the filter must have a full-cycle data window length which leads to one cycle delay in the DVR response. Thus, a compromise between the voltage injection speed and disturbance attenuation is made. The designed LES filters utilize a data window length of 50 samples at the sampling rate of 10 kHz and, hence, estimate the voltage phasor parameters in 5 ms depicts the frequency response of the LES filters and indicates significant attenuation of voltage noise, harmonics, and distortions at frequencies higher than 200 Hz and lower than 50 Hz. demonstrates the effectiveness of this filter in attenuating the noise, harmonics, and distortions for the sag compensation mode of operation as well. The next section shows that this filter also performs satisfactorily in the FCI operation mode, even under arcing fault conditions where the measured voltage and current signals are highly distorted.

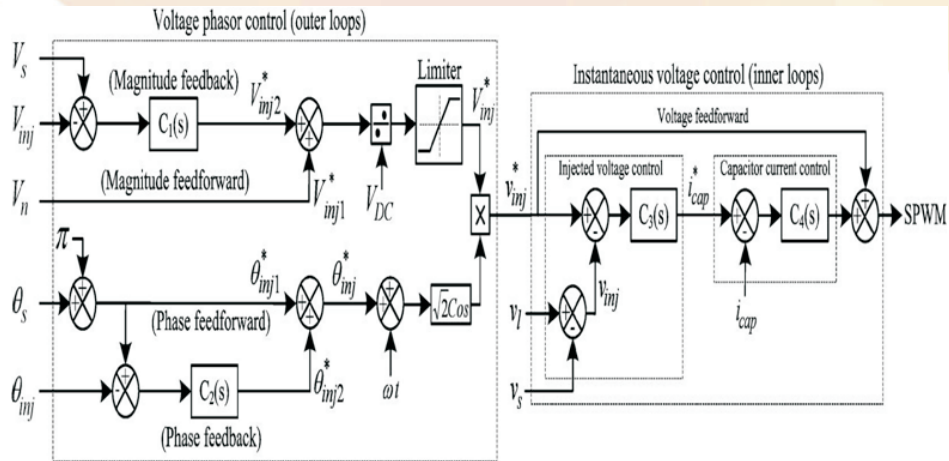


Fig.7: Per-Phase Block Diagram of DVR.

Fig.7 shows a per-phase block diagram of the proposed DVR control system corresponding to the FCI operation mode where  $V_s$  is the nominal r.m.s phase voltage. The control system of Fig. 2 utilizes  $V_s$ ,  $V_L$ , the dc-link voltage  $V_{DC}$ , and the harmonic filter capacitor current  $i_{cap}$  as the input signals. The reported studies in this paper are based on the over current fault detection method of [7] and [12]. The fault detection mechanism for each phase is activated when the absolute value of the instantaneous current exceeds twice the rated load current.

The proposed multi loop control system [3], includes an outer control loop (voltage phasor control) and an inner control loop (instantaneous voltage control). The inner loop provides damping for the transients caused by the DVR harmonic filter and , and improves the dynamic response and stability of the DVR. The inner loop is shared by the sag compensation and the FCI functions. When a downstream fault is detected, the outer loop controls the injected voltage magnitude and phase angle of the faulty phase(s) and reduces the load-side voltage to zero, to interrupt the fault current and restore the PCC voltage. The DVR “outer” voltage phasor control and “inner” instantaneous voltage control, corresponding to each phase, are described in the following two subsections.

**VOLTAGE PHASOR CONTROL SYSTEM:**

In the FCI operation mode, the required injected voltage phasor is equal to the source voltage phasor, but in phase opposition. Performance of the voltage phasor control.

In terms of transient response, speed, and steady-state error, is enhanced by independent control of voltage magnitude and phase, and incorporating feed forward signals to the feedback control system Fig. 2 shows two proportional-integral (PI) controllers ( $C_1$  and  $C_2$ ) that are used to eliminate the steady-state errors of the magnitude and phase of the injected voltage, respectively. Parameters of each controller are determined to achieve a fast response with zero steady-state error. The magnitude and the phase angle of are independently calculated and the magnitude is passed through a limiter (Fig. 2). The resulting phasor magnitude and phase angle are converted to the sinusoidal signal  $\vec{V}^*$ , which is the reference signal for the instantaneous voltage control.

**INSTANTANEOUS VOLTAGE-CONTROL SYSTEM:**

Under ideal conditions, voltage sag can be effectively compensated if the output of the phasor – based controller is directly fed to the sinusoidal pulse width modulation (SPWM), Unit. However resonance of the harmonic filter cannot be eliminated under such conditions. Therefore, to improve the stability and dynamic response of the DVR, an instantaneous injected voltage controller and a harmonic filter capacitor current controller are used to attenuate resonances.



A Large KV results in amplification of the DVR filter resonance and can adversely impact the system stability [18]. Thus, the transient response of the DVR is enhanced by a feed forward loop, and a small proportional gain is utilized as the voltage controller. A large  $K_p$  damps the harmonic filter resonance more effectively, but it is limited by practical considerations (e.g., amplification of capacitor current noise, measurement noise, and dc offset ). Therefore, the lowest value of the proportional gain which can effectively damp the resonances is utilized. The output of the current controller is added to the feed-forward voltage to derive the signal for the PWM generator.

**INSTANTANEOUS VOLTAGE-CONTROL SYSTEM:**

Under ideal conditions, voltage sag can be effectively compensated if the output of the phasor – based controller is directly fed to the sinusoidal pulse width modulation (SPWM), Unit. However resonance of the harmonic filter cannot be eliminated under such conditions. Therefore, to improve the stability and dynamic response of the DVR, an instantaneous injected voltage controller and a harmonic filter capacitor current controller are used to attenuate resonances.

A Large KV results in amplification of the DVR filter resonance and can adversely impact the system stability [18]. Thus, the transient response of the DVR is enhanced by a feed forward loop, and a small proportional gain is utilized as the voltage controller. A large  $K_p$  damps the harmonic filter resonance more effectively, but it is limited by practical considerations (e.g., amplification of capacitor current noise, measurement noise, and dc offset ). Therefore, the lowest value of the proportional gain which can effectively damp the resonances is utilized. The output of the current controller is added to the feed-forward voltage to derive the signal for the PWM generator.

| Parameter                                   | Value                |
|---|----------------------|
| Grid voltage (L-L) (rms) $V_{base}$         | 415 V                |
| Line frequency                              | 50 Hz                |
| Nominal PV power (Base kVA)                 | 10 kVA               |
| Nominal load power                          | 10 kVA               |
| Nominal load power factor                   | 0.8 lagging          |
| DC link voltage                             | 700 V                |
| DC link capacitance                         | 3000 $\mu$ F         |
| Maximum shunt current, ( $I_{sh-max}$ )     | 20 A                 |
| Series transformer rating/turn ratio        | 10 kVA/ 1:1          |
| Filter inductor $L_f$ and capacitance $C_f$ | 5 mH and 50 $\mu$ F  |
| Grid impedance $Z_{line}$                   | $0.5 + j0.05 \Omega$ |

System parameters used in simulation reference frame as shown in fig.7

**V. SIMULATION STUDY**

In this section, MATLAB/Simulink-based study is presented to illustrate the feasibility of proposed system configuration. Here two reference signals can be expressed in both PV-VSI and DVR-VSI reference signals, and determined by their control blocks determined in earlier section.

**THREE PHASES DOWNSTREAM FAULT INTERRUPTION WITH DVR.:**

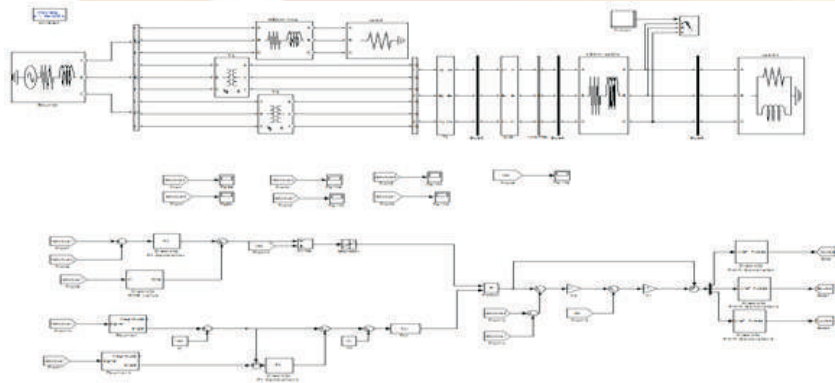


Fig.9:Simulation block diagram of three phases downstream fault Interruption with DVR.

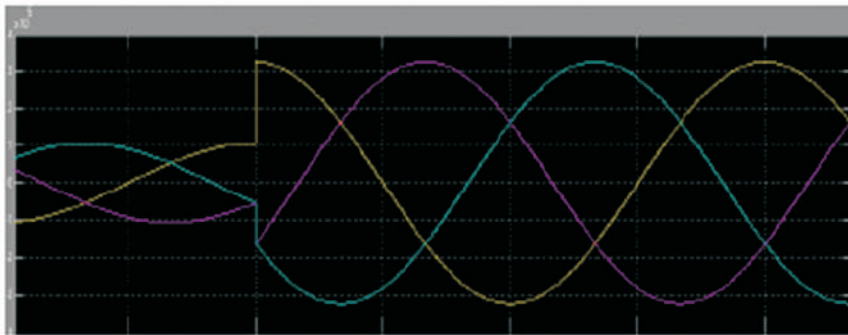


Fig.10: Injected voltage with time on x-axis and voltage on y-axis.

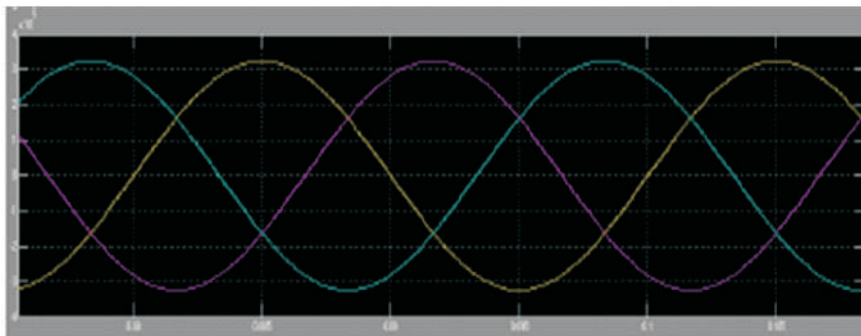


Fig.11:Supply voltage with time on x-axis and voltage on y-axis.

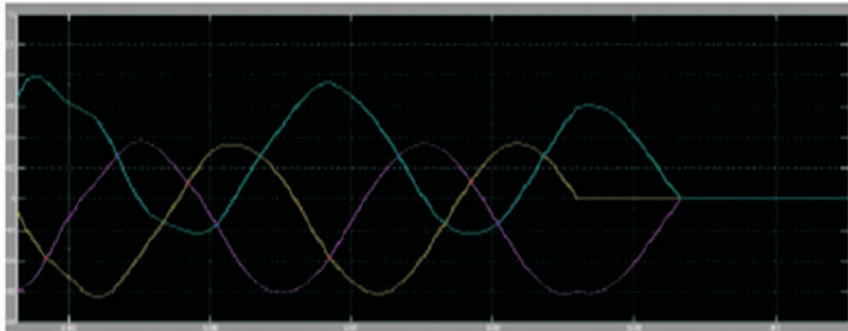


Fig.12: Line current with time on x-axis and current on y-axis.

During Mode types like Healthy grid mode, Fault mode, sag mode and No PV generation mode corresponds to the interval depending on their active and reactive power. It is some sot of difficult in balanced three phase and unbalanced modes of operation.

### ANALYSIS OF STUDY:

A small drop in voltage and small jump in phase angle can be tolerated by the load itself. If the voltage magnitude lies between 90%–110% of nominal voltage and 5%–10% of nominal state that will not disturb the operation characteristics of loads. Both magnitude and phase are the control parameter for this method which can be achieved by small energy injection. We will begin this section with a broad overview, covering the “high-level” operation of one form of the discrete filter (see the previous footnote). After presenting this high-level view, we will narrow the focus to the specific equations and their use in this version of the filter. The filter estimates a process by using a form of feedback control: the filter estimates the process state at some time and then obtains feedback in the form of (noisy) measurements. As such, the equations for the filter fall into two groups: time update equations and measurement update equations. The time update equations are responsible for projecting forward (in time) the current state and error covariance estimates to obtain the a priori estimates for the next time step. The measurement update equations are responsible for the feedback—i.e. for incorporating a new measurement into the a priori estimate to obtain an improved a posteriori estimate. The time update equations can also be thought of as predictor equations

### VI. CONCLUSION

In this paper, a brand new process configuration for integrating a conventional grid-connected PV method and self supported DVR is proposed. The proposed configuration now not best reveals the entire functionalities of present PV and DVR method, but also enhances the DVR working range. It permits DVR to utilize energetic power of PV plant and for that reason improves the process robustness towards sever grid faults. The proposed configuration can operate in unique modes established on the grid and PV power generation. The mentioned modes are healthy grid mode, fault mode, sag mode, and PV inactive mode. The excellent simulation learns and experimental validation demonstrates the effectiveness of the proposed configuration and its useful feasibility to perform beneath one-of-a-kind operating stipulations. The proposed configuration could be very useful for contemporary load centers the place on-web page PV iteration and strict voltage regulations are required.

### REFERENCES

1. R. A. Walling, R. Saint, R. C. Dugan, J. Burke, and L. A. Kojovic, “Summary of distributed resources impact on power delivery systems,” *IEEE Trans. Power Del.*, vol. 23, no. 3, pp. 1636–1644, Jul. 2008.
2. Meza, J. J. Negroni, D. Biel, and F. Guinjoan, “Energy-balance modeling and discrete control for single-phase grid-connected PV central inverters,” *IEEE Trans. Ind. Electron.*, vol. 55, no. 7, pp. 2734–2743, Jul. 2008.
3. T. Shimizu, O. Hashimoto, and G. Kimura, “A novel high-performance utility-interactive photovoltaic inverter system,” *IEEE Trans. Power Electron.*, vol. 18, no. 2, pp. 704–711, Mar. 2003.
4. S. B. Kjaer, J. K. Pedersen, and F. Blaabjerg, “A review of single-phase grid-connected inverters for photovoltaic modules,” *IEEE Trans. Ind. Appl.*, vol. 41, no. 5, pp. 1292–1306, Sep./Oct. 2005.
5. T. Esmar, J. W. Kimball, P. T. Krein, P. L. Chapman, and P. Midya, “Dynamic maximum power point tracking of photovoltaic arrays using ripple correlation control,” *IEEE Trans. Power Electron.*, vol. 21, no. 5, pp. 1282–1291, Sep. 2006.
6. IEEE Recommended Practices and Requirements for Harmonic Control in Electrical Power Systems, IEEE Standard 519–1992, Apr. 1993, pp. 1–112. [7] J. A. Martinez and J. M. Arnedo, “Voltage sag studies in distribution networks—Part I: System modeling,” *IEEE Trans. Power Del.*, vol. 21, no. 3, pp. 338–345, Jul. 2006.
7. J. D. Li, S. S. Choi, and D. M. Vilathgamuwa, “Impact of voltage phase jump on loads and its mitigation,” in *Proc. 4th Int. Power Electron. Motion Control Conf.*, Xian, China, Aug. 14–16, 2004, vol. 3, pp. 1762–1766.